Accepted Manuscript

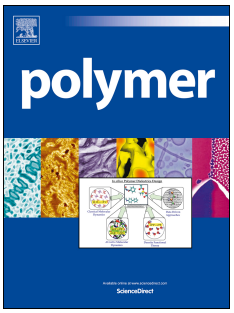

Macromolecular iron-chelators via RAFT-polymerization for the inhibition of methicillin-resistant *Staphylococcus aureus* growth

Junpei Li, Eniola D. Olaleye, Xiaole Kong, Tao Zhou, Yongmin Ma, Jagoda Jurach, Osamah Al Rugaie, Robert C. Hider, Guoqing Zhang, Selwa Alsam, Vincenzo Abbate

PII: S0032-3861(16)30073-8

DOI: 10.1016/j.polymer.2016.01.073

Reference: JPOL 18425

To appear in: *Polymer*

Received Date: 29 September 2015

Revised Date: 23 January 2016

Accepted Date: 27 January 2016

Please cite this article as: Li J, Olaleye ED, Kong X, Zhou T, Ma Y, Jurach J, Al Rugaie O, Hider RC, Zhang G, Alsam S, Abbate V, Macromolecular iron-chelators via RAFT-polymerization for the inhibition of methicillin-resistant *Staphylococcus aureus* growth, *Polymer* (2016), doi: 10.1016/j.polymer.2016.01.073.

Polymeric iron scavengers deprive MRSA organisms of essential iron

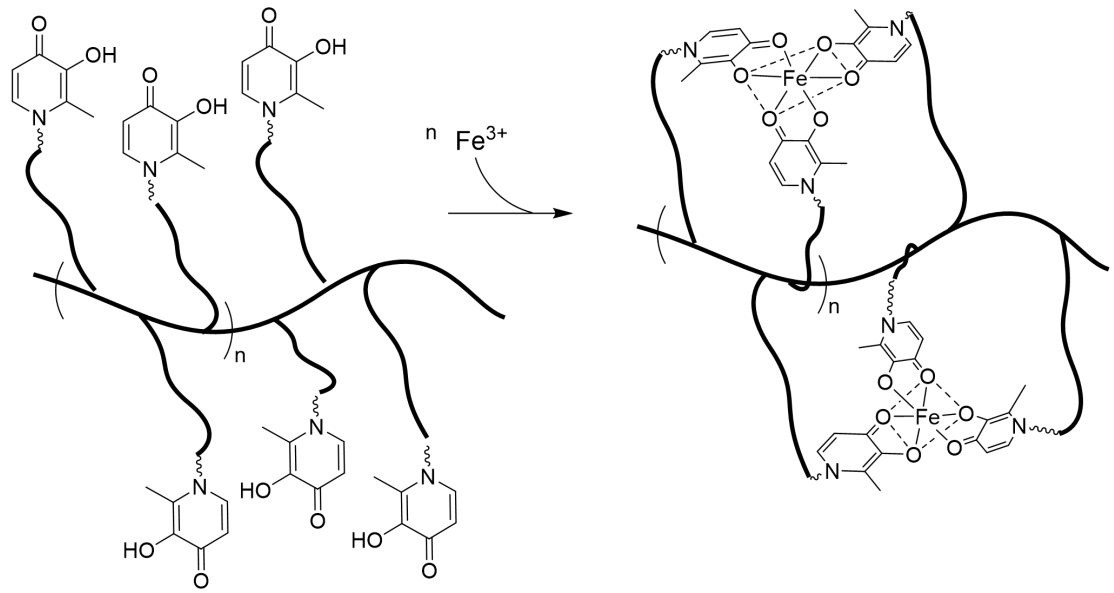

Macromolecular Iron-Chelators via RAFT-Polymerization for the Inhibition of Methicillin-Resistant *Staphylococcus aureus* Growth

Junpei Li[a], Eniola D. Olaleye[b], Xiaole Kong[c], Tao Zhou[d], Yongmin Ma[e], Jagoda Jurach[c], Osamah Al Rugaie[b,f], Robert C. Hider [c], Guoqing Zhang[a*], Selwa Alsam[b] and Vincenzo Abbate[c*]

[a] Hefei National Laboratory for Physical Sciences at the Microscale, University of Science and Technology of China, Hefei, Anhui, 230026, P. R. China.

[b] School of Biological Sciences, University of Essex, Wivenhoe Park, Colchester, CO4 3SQ, UK

[c] Institute of Pharmaceutical Science, King's College London, Franklin-Wilkins Building, 150 Stamford Street, London, SE1 9NH, UK.

[d] School of Food Science and Biotechnology, Zhejiang Gongshang University, 18 Xuezheng Street, Hangzhou, Zhejiang, 310018, P. R. China.

[e] Zhejiang Chinese Medical University, 548 Binwen Road, Hangzhou, 310053, P R China.

[f] Unizah College of Medicine and Medical Sciences (UCM), Qassim University, P.O. Box 991, AlQassim 51911, Saudi Arabia.

Abstract: A series of linear poly (glycidyl methacrylate) (PGMA) polymers were synthesized via RAFT polymerization and conjugated with amine-containing 3-hydroxypyridin-4-ones (HPOs) to generate a panel of HPO-containing materials with controlled structures and specific iron-binding functions. The structures of the resulting polymers were characterized via ^{1}H-NMR, GPC and FT-IR and their chelating capacity for iron was investigated using UV-Vis spectrophotometric titration of the iron(III) complexes. *In vitro* antimicrobial studies of selected ligand-containing homopolymers demonstrate that the homopolymers are capable of inhibiting the growth of methicillin-resistant *Staphylococcus aureus* (MRSA). It is proposed that the inhibition activity of MRSA is derived from the iron-chelating capability of the iron-binding polymers.

Keywords: MRSA; Hydroxypyridinones; Iron-binding polymers.

1. Introduction

In recent years, macromolecular iron chelators have received increasing attention as human therapeutic agents.[1, 2] Polymeric chelators have been used for water treatment,[3] pollution control,[4] recovery of metals,[5, 6] active packaging[7, 8] and analytical chemistry.[9, 10] Recently several iron binding polymer applications in the biomedical field have been reported.[11] As iron is an essential element for all living processes, in principle targeting iron is a useful approach for the treatment of microbial infectious diseases.[12, 13] Macromolecular iron chelators also have potential in the treatment of acute iron overload.[14] Although most of the present-day iron-chelating therapeutic agents are designed as small molecules, there are a number of advantages associated with polymeric therapeutics that cannot be readily achieved with low molecular weight drugs. For example, when taken orally, the high-molecular-weight characteristic of polymers render them largely non-absorbed by the gastrointestinal tract, thus potentially extending the drug half-life.[1]

The design of iron chelating polymers is presently based on several strategies, one involving the immobilization of natural chelators (e.g., desferrioxamine B) onto activated supports[15, 16], a second involving the conjugation of bidentate ligands with activated polymers[17, 18] and a third, copolymerization of 1-(-acrylamidoethyl)-3-hydroxy-2-methyl-4(1*H*)-pyridinone (AHMP) with other cross-linking agents.[19] The former structures are presently limited to carbohydrate matrices and, as a consequence, are expensive to prepare, and high binding capacities are difficult to achieve. Furthermore the synthetic chemistry for the second and third approaches is difficult to control, generating polydisperse polymers and crosslinked materials with poor solubility. It is therefore desirable to develop a simple preparative method for iron-binding polymers of well-defined structure.

Poly(glycidyl methacrylate) (PGMA) is a well-known polymer for both industrial and biomedical applications because it is reactive, inexpensive, hydrophilic, biocompatible, and generally nontoxic. Furthermore it permits fast and efficient post-polymerization modifications.[20, 21] RAFT polymerization was successfully employed for the synthesis of well-defined PGMA polymers, exerting remarkable control over their molecular weight and affording polymers with low polydispersities.[22, 23] Recently, both linear- and star-shaped PGMAs were

modified with different amines by a nucleophilic ring-opening reaction of the epoxy group.[24, 25] 3-Hydroxypyridin-4-ones (HPOs) are one of the main classes of candidates for the development of clinically useful iron chelators, and 1,2-dimethyl-3-hydroxypyridin-4-one (deferiprone, Figure 1) is currently available for clinical use (Apotex Inc., Toronto, Canada as Ferriprox).[26] We therefore sought to utilize amine-containing HPOs, such that the amine functionality can be subsequently added onto a pre-formed PGMA, in a ring-opening process to obtain novel macromolecular iron chelators.

1.1 Iron restriction and Staphylococcus activity

Staphylococcus aureus is a widespread and dangerous pathogen that is responsible for many human infections worldwide.[27] Some characteristics that help account for the prevalence of *S. aureus* as a human pathogen include its genetic diversity, ability to acquire new exogenous genes, a remarkable propensity to acquire resistance to multiple antimicrobial agents, high virulence and efficient quorum sensing mechanisms.[28] *S. aureus* infections range from moderately severe infections of the skin or the respiratory tract to life-threatening diseases such as necrotizing pneumonia, necrotizing fasciitis, osteomyelitis, endocarditis and toxic shock syndrome.[29, 30] These infections impose a high and increasing burden on healthcare resources[31] and are associated with high morbidity and mortality[32] as well as a longer hospital stay.[33, 34]

The global spread of methicillin-resistant *S. aureu*s (MRSA) has become one of the most serious contemporary challenges to the treatment of hospital-acquired infections (HAIs).[35] MRSA bear the *mecA* gene that encodes a 78-kDa penicillin-binding protein 2a (PBP2a) which has low-affinity for methicillin and all β-lactam antibiotics.[29] MRSA is the principal cause of nosocomial infections caused by a single bacterial pathogen in the United States and many other parts of the world.[36-39] An estimated 44% of all HAIs can be attributed to MRSA.[40] Furthermore, the emergence and dramatic increase of MRSA infections in otherwise healthy individuals with no risk factors has become an issue of increasing concern.[41]

MRSA has acquired resistance to multiple antibiotic classes and this has limited the therapeutic options available for its treatment.[41, 42] Vancomycin is considered

the workhorse of parenteral anti-infective agents for MRSA, yet, some strains of *S. aureus* exhibit reduced susceptibility to vancomycin.[43-45] Many of the new antimicrobial agents available for the treatment of MRSA infections (e.g. linezolid, quinupristin-dalfopristin, daptomycin, tigecycline and telavancin) are associated with dose-limiting adverse events, emerging resistance issues, and high cost.[46] This emphasizes the need for further research to identify new antimicrobial drug targets in MRSA as well as to develop new antimicrobial agents with novel mechanisms of action against MRSA.

All microorganisms require iron for both growth and replication. Most microorganisms have developed efficient methods of absorbing iron from the environment and many microorganisms secrete siderophores in order to scavenge iron. The role of these compounds is to scavenge iron from the environment and render it available to the microbial cell. Hence, limiting the amount of available iron should, in principle, inhibit microbial growth. It has been established that both bidentate and hexadentate iron chelators can control the growth of a wide variety of microorganisms.[47, 48] In this work we have investigated the possible application of polymeric bound chelators on the growth of S. *aureus*. Thus, the synthesis of a panel of HPO bidentate ligands with different amine-substituents and PGMA of two molecular weights, as well as the post-polymerization modification by nucleophilic ring-opening reaction of the epoxy group is reported. For the first time, RAFT polymerization[49, 50] has been employed to generate well-defined polymeric HPO-based macromolecular chelators. The physicochemical properties of the monomer bidentate ligands and the iron-chelating properties of the resultant PGMA-HPO chimera have been investigated. Preliminary *in vitro* antimicrobial activity against MRSA is reported.

2. Materials and methods

2.1 Materials

All chemicals were purchased from Aldrich or Merck Chemical Company and used without any further purification. Column chromatography purifications were performed on Merck silica gel 60 (0.04−0.063 mm). ^{1}H NMR and ^{13}C NMR spectra were recorded using a Bruker Avance 400 (400 MHz) NMR spectrometer. Chemical shifts (δ) are reported in ppm downfield from the internal standard tetramethylsilane

(TMS). J values are in hertz (Hz), and splitting patterns are designated as follows: s (singlet), bs (broad singlet), d (doublet), t (triplet), and m (multiplet). The ESI-MS analyses were performed using a Waters/Micromass ZQ mass spectrometer (Manchester, UK). HRMS were carried out by the Mass Spectrometry Facility, School of Biomedical and Health Science, King's College London. Purity was determined via HPLC analysis.

2.2 Polymerization of glycidyl methacrylate (GMA)

The following conditions were used for the synthesis of PGMA using [GMA]/[CPBD] ratios of 65:1 and 100:1, in anhydrous toluene, at 62 °C. A solution of GMA (4.9 g, 3.43×10^{-2} mol, 65 equiv.), CPBD (11.6×10^{-2} g, 5.28×10^{-4} mol, 1.0 equiv.), and AIBN (2.9×10^{-2} g, 1.76×10^{-4} mol, 0.33 equiv.) or a solution of GMA (5.0 g, 3.52×10^{-2} mol, 100 equiv.), CPBD (7.8×10^{-2} g, 3.52×10^{-4} mol, 1.0 equiv.), and AIBN (1.9×10^{-2} g, 1.17×10^{-4} mol, 0.33 equiv.) were prepared to obtain the [GMA]/[CPBD] ratios of 65:1 or 100:1, respectively. The solutions were degassed using three freeze-pump-thaw cycles to remove traces of oxygen. The Schlenk tubes were placed in an oil bath preheated at 62 °C and the polymerizations were carried out for 5hrs and 2hrs, respectively. After completion, the polymerization mixture was precipitated into ethyl ether to remove the unreacted monomer followed by filtration and drying under vacuum. Monomer to polymer conversions was determined by ^{1}H NMR spectroscopy of the samples taken from the polymerization mixture at different time intervals. The products were characterized by GPC and ^{1}H NMR. DMF (*N*,*N*-Dimethylformamide) GPC analysis coupled to a refractive-index detector (vs. PS standards) indicated a M_n of 12,800 g mol^{-1} and an M_w/M_n of 1.07 for **7**, and an M_n of 9,300 g mol^{-1} and an M_w/M_n of 1.07 for **8**.

2.3 Synthesis of iron-binding polymers

For the preparation of an iron-binding polymer using **1** or **3** as the amine-containing HPO ligands, 0.2 g of PGMA (**7** or **8**) and 1 mL of triethylamine were dissolved in 8 mL of DMF. The reaction mixture was stirred at 55 °C for 36 h to produce **7.1**, **8.1**, **7.3** and **8.3**. The final reaction mixture was precipitated with excess diethyl ether and the resulting polymer-drug conjugate was purified via dialysis for

three days against excess distilled water with frequent water changes. For the preparation of iron-binding polymers using HPOs **2**, **4**, **5** or **5b**, 0.2 g of PGMA (**7** or **8**) was dissolved in 8 mL of DMF. **2**, **4**, **5** or **5b** and 1 mL of triethylamine were then added. The reaction mixtures were stirred at 80 °C for 2 h to produce polymers **7.2**, **8.2**, **7.4, 8.4**, **7.5, 8.5** and **7.5b**. The final reaction mixtures were precipitated with excess diethyl ether and the resulting polymer-drug conjugates were purified via dialysis for three days as described above. **7.4** and **8.4** were found to be insoluble in all solvents investigated. **7.5b**, **7.5**, **8.5**, **7.3** and **8.3** were soluble in DMSO: H_2O (1:1, v/v). The M_n of the conjugated products was calculated as derived from the estimated M_n (NMR) of the corresponding PGMA and assuming 100% conjugation of the epoxide ring-opening reactions, as judged by ^{1}H NMR and FT-IR data.

2.4 pKa determination

Equilibrium constants of protonated ligands were determined using an automated computerized system, consisting of a UV/vis spectrophotometer (Perkin-Elmer Lambda 5), an autoburette (Metrohm Dosimat 665), a pH meter (Corning Delta 225), and a peristaltic pump (Watson-Marlow 101U/R M2) all interfaced to a computer. A blank titration of 0.1 M KCl (20 mL) was carried out to determine the electrode zero and slope using GLEE.[49] The solution (0.1 M KCl, 20 mL), contained in a jacketed titration cell, was acidified by the addition of 0.15 mL of 0.2 M HCl. Titration was carried out against 0.3 mL of 0.2 M KOH using 0.01 mL increments dispensed from the dosimat. All solutions were maintained at 25 ± 0.5 °C under an argon atmosphere. The above titration was repeated in the presence of bidentate ligands. The data obtained from titration were analyzed using the pHab software.[52]

2.5 Determination of stability constant of the iron(III) complex with bidentate ligands

In a typical experiment, iron(III) (35.9 µM) and bidentate ligand (180 µM) in 0.1 M KCl (20 mL) were alkalimetrically titrated from pH 1.6 to 7.6 at 25 ^{o}C. Each pH observation was taken after standing for 30 minutes to achieve equilibrium. The titration data were analyzed using pHab software.[52] The affinity constants were used to provide pFe^{3+} values for the following conditions: $[Fe^{3+}]_{total}$ = 1 µM, [ligand]

$_{total}$ = 10 µM, pH =7.4. A typical spectral series for compound **1** is presented in Figures S1 and S2 (SI).

2.6 Chelating capacity of iron(III)-binding homopolymers

Dry chelating homopolymer (**7.1,** 4.25 mg, or 6.15 mg, **8.5**) was added to 0.4 mL DMSO to prepare a stock solution. 5 µL aliquots of the above stock solution were added to 1.4 mL water to yield the final solution to be assayed (the concentrations of homopolymers **7.1** and **8.5** were 0.75 and 6.15 µM, respectively). Iron(III) aqueous solution (0.8953 mM, $FeCl_3$) was placed in a stoppered vessel ready for titration. Batch spectrophotometric determinations were performed on a UV spectrophotometer scanning from 250 to 600 nm. Automatic titration and spectral scans adopted the following strategy: 5 µL iron solution was added for each point, until absorbance remained unchanged for 30 min.

2.7 Preparation of polymers for antimicrobial activity determination

Stock solutions of polymers used in this study were prepared by dissolving in different solvents as appropriate e.g. 20% DMSO in water for **7.1** and 50% DMSO in water for **7.5** and **7.5b**.

2.8 Bacterial culture

One strain of MRSA (a nasal isolate obtained from the Colchester Hospital University Foundation NHS Trust) was used in this study. MRSA was inoculated in 10 mL Luria-Bertani (LB) broth medium and cultured without shaking at 37 ^{o}C in aerobic conditions for 6 hours. Optical Density (OD) was measured at wavelength 595 nm to give a colony forming unit (CFU)/mL of ~10^8 (OD_{595} 0.22 = ~10^8 CFU/mL). The reference strains MRSA NCTC 12493 and *S. aureus* NCTC 6571 were used in this study.

Antibiotic susceptibility testing

The susceptibility of the MRSA isolate used in this study to a number of antibiotics (as listed in Table 3 in result section) was determined using the disk diffusion (Kirby-Bauer) method. The OD of a 6 hr broth culture of the isolate was adjusted to within the range of >0.1 - 0.3 at wavelength 500 nm in a spectrophotometer. 40 µl of

the standardized culture was then added to 5 ml sterile distilled water following which sterile swab sticks were dipped into the bacterial suspension and swabbed on the entire surface of nutrient agar plates. Plates were left to dry for about 5 mins following which antibiotics were placed on the surface of the nutrient agar plates. All plates were then incubated at 37 ^{o}C for 18 hrs. The zones of inhibition around the antibiotic discs were measured and the results interpreted as resistance or susceptible based on the interpretative standard of the British Society for Antimicrobial Chemotherapy - BSAC (BSAC, 2015).

Identification of the MRSA isolate

PCR was done in order to confirm the identity of the MRSA isolate used in this study. DNA was extracted using the QIAamp DNA Mini kit (QIAGEN) according to manufacturer's instructions. To confirm that the isolate was *S. aureus*, primers nuc1 and nuc2 were used in PCR to amplify the *S. aureus*-specific thermonuclease (nuc) gene. PCR amplification consisted of a 5 min initial denaturation step at 95 ^{o}C followed by 37 cycles of denaturation at 95 ^{o}C for 30 secs, annealing at 55 ^{o}C for 30 secs and extension at 72 ^{o}C for 60 secs, with a final extension step at 72 ^{o}C for 10 mins. Furthermore, primers mec1 and mec2 and specific to a 162 bp region of DNA specific to the *mecA* gene were used in PCR to confirm that the isolate was indeed MRSA. PCR amplification consisted of a 4 min initial denaturation step at 94˚C followed by 35 cycles of denaturation at 94 ^{o}C for 30 secs, annealing at 53˚C for 30 secs and extension at 72 ^{o}C for 1 min, with a final extension step at 72˚C for 4 min.

Agarose gel electrophoresis

PCR products and extracted DNA were analysed in 1% agarose gels to which SafeView nucleic acid stain (nbs biologicals) had been added for fluorescent visualisation of DNA bands. Gels were run in 1X TAE electrophoresis buffer at 150 V for 15 mins in a Mini-Sub cell GT electrophoresis apparatus (Bio-Rad) were visualised in a Syngene InGenius^{3} gel documentation system.

2.9 Antimicrobial assay

The incubation medium was water and all assays were performed in 96-well plates with ~10^7 CFU/mL of bacteria per well in the absence or presence of different concentrations of the polymers. Plates were incubated at 37 ^{o}C under aerobic conditions for 24 hours after which the number of viable bacteria in each well was determined by their growth on Cysteine Lactose Electrolyte Deficient (CLED) agar. The bactericidal rate was calculated as follows:

$$(R = \frac{[X_0 - X_t]}{X_0} \times 100)$$

where R is the bactericidal rate, X_0 the number of bacteria without polymer (control), and X_t the number of bacteria after the treatment with polymer. Minimum inhibitory concentration (MIC) endpoints were determined as the lowest concentration of the antimicrobials that inhibited the visible growth of bacteria after 24 hours incubation using the micro-dilution method recommended by the British Society for Antimicrobial Chemotherapy (BSAC)[53]. Measurements were carried out in triplicate.

3. Results and discussion

3.1 Chemistry

The 1-substituted-2-methyl-3-hydroxy-4(1*H*)-pyridinones in this study (**1-4,** Figure 1) were synthesized utilizing the methodology described by Dobbin and co-workers[54, 55] (Schemes S1-S3 in the SI). The commercially available 2-methyl-3-hydroxy-4(1*H*)-pyranone, maltol, was benzylated in 90% aqueous methanol to give 3-(benzyloxy)-2-methyl-4*H*-pyran-4-one (**1a**).[56] 3-Methoxy-2-methyl-5-((methylamino)methyl)pyridin-4(1*H*)-one (**5a**) was readily prepared from commercially available maltol in a four-step reaction by following an established procedure.[57] The resulting protected HPO was found to partition from aqueous solution (pH 7) into chloroform and was finally purified by column chromatography. **2a** was synthesized according to a reported procedure[58] and protected via the Mannich reaction. Removal of the protecting benzyl group was achieved by catalytic hydrogenolysis invariably to yield the corresponding bidentate chelators as the free bases. The bidentate ligand **5** was obtained after removal of methyl groups by treatment of **5b** with boron trichloride. The final bidentate ligands

(**1-5**, Schemes S1-3 in the SI and Figure 1) were obtained as a pale-yellow solid or a brown oil, and characterized using ^{1}H, ^{13}C NMR, and high-resolution mass spectroscopy. The purity of the compounds was determined by analytical RP-HPLC using a C18 column. The protected intermediate **5b** was employed to prepare a control polymer **7.5b**, thus not possessing iron-chelating ability.

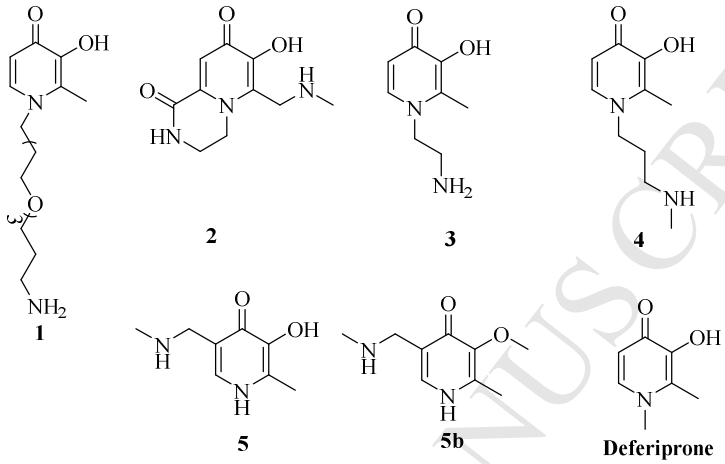

Figure 1. Structure of bidentate ligands.

Glycerol monomethacrylate (GMA) was polymerized in anhydrous toluene at 62 °C using an azo initiator (AIBN) and a dithiobenzoate-based RAFT agent (CPBD) to produce well-defined RAFT PGMA with epoxy functionalized groups that enabled further post-polymerization modifications. GPC was used to determine M_n and PDI values for PGMA **7** and **8**. As expected by the RAFT technology, nearly monodisperse materials were obtained. As a consequence, it was assumed that the subsequent conjugation with amine-HPOs would yield well-defined macromolecular iron chelators. The bidentate ligands **1-5** were used as nucleophilic reagents to perform ring-opening reactions of PGMA to yield the final RAFT-based iron-binding polymers (Scheme 1). According to the HPO used, we were able to produce a panel of polymers with various properties (Table 1). Conjugation of PGMA with primary and secondary amine-containing HPOs (e.g. **3** and **4**) resulted in materials with either poor water solubility (**7.3** and **8.3**) or with general insolubility properties (**7.4** and **8.4**); clearly, removal of hydrogen bonding capability when transforming a primary amine (**3**) to a secondary amine (**4**) markedly decreased the solubility of the resultant macromolecular chelators. Using **5**, as slightly more hydrophilic HPO-ligand, yielded

polymers **7.5** and **8.5** with improved solubility in aqueous DMSO solutions. This prompted the design of compound **1** (Figure 1) in order to produce the more hydrophilic polymers **7.1** and **8.1** which possessed good water solubility properties. In order to prepare a control polymer with similar macromolecular structure to that of **7.5**, we employed the protected intermediate **5b** to produce polymer **7.5b**, which lacked iron-chelating ability due to methylation of the 3-hydroxyl group on the HPO ring. For the polymer-**7** series, the number of chelating units per polymer chain is 106; the corresponding number for the polymer-**8** series is 28.

Table 1. Physical properties of iron-binding polymers[1].

Polymer	PGMA	Ligand	Solubility	M_n [2]
7.5b	**7**	**5b**	H_2O/DMSO (1:1, v/v)	34,700
7.1	**7**	**1**	H_2O	50,100
7.2	**7**	**2**	H_2O/DMSO (1:1, v/v)	38,900
7.3	**7**	**3**	H_2O/DMSO (1:1, v/v)	33,100
7.4	**7**	**4**	None	36,100
7.5	**7**	**5**	H_2O/DMSO (1:1, v/v)	33,100
8.1	**8**	**1**	H_2O	13,400
8.2	**8**	**2**	H_2O/DMSO (1:1, v/v)	10,400
8.3	**8**	**3**	H_2O/DMSO (1:1, v/v)	8,900
8.4	**8**	**4**	None	9,700
8.5	**8**	**5**	H_2O/DMSO (1:1, v/v)	8,900

[1] For the polymer **7** series, the number of chelating units per polymer chain has been calculated to be 106; the corresponding figure for the **8** series is 28.

[2] The M_n of iron-binding polymers was derived from the calculated PGMA M_n and assuming a quantitative conjugation of the HPO ligand to the PGMA epoxide units.

To demonstrate the versatility of this synthetic approach, we designed compound **2** as a nucleophilic ligand to prepare fluorescent polymer-chelator chimera (**7.2** and **8.2**) where drug and fluorophore were embedded in the same structural unit. This

strategy was preferred to the conventional approach to the preparation of fluorescent RAFT polymers.[59, 60] Such methods usually make use of post-polymerization chemistries to transform the RAFT agent into a fluorophore. Our approach was therefore faster, producing multifluorescent moieties per polymer chain. Fluorescent spectra confirmed the fluorescent properties of both compound **2** and the resultant polymers **7.2** and **8.2** (SI, Figures S9-S11). These polymers will be useful to establish their cellular localization in future microbial studies.

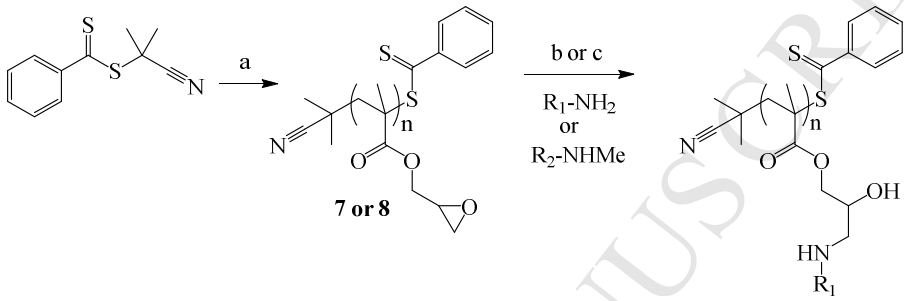

Scheme 1. Synthesis of PGMA and iron-binding polymers[1, 2]

(a) AIBN and GMA; 62 ^{o}C, toluene; (b) 55 ^{o}C, DMF, 36h; (c) 80 ^{o}C, DMF, 2h.

[1] Polymer nomenclature: **X.Y**, where **X** is the parent PGMA and **Y** is the conjugated HPO

[2] For **7.3** and **8.**3, R_1 = **3**; for **7.1** and **8.1**, R_1 = **1**; for **7.5** and **8.5**, R_2 = **5**; for **7.2** and **8.2**, R_2 = **2**; for **7.4** and **8.4**, R_2 = **4**; and for **7.5b**, R_2 = **5b**.

GPC analysis under various conditions (water, DMF or their mixtures) was not found to be practical for the HPO-PGMA conjugates; therefore the final M_n of conjugates was estimated by assuming a 100% epoxide ring-opening reaction, as confirmed by FT-IR and ^{1}H NMR data. Figure S3 (SI) shows the ^{1}H NMR spectra of the PGMA, which reveals that the epoxy ring remained intact during the polymerization reaction. The peaks at δ = 7.44 – 8.14 ppm correspond to the aromatic protons of the CPBD units, indicating that the resulting RAFT polymers had incorporated the chain-transfer agent. The peaks at δ = 3.23 ppm, 2.63 and 2.83 ppm can be assigned to the protons of the oxirane ring. The two protons were in different chemical environments, resulting in two different resonances. End-group analysis was used to calculate the mean degree of polymerization (DP) for this reaction, polymer **7** with a DP of 106 and M_n = 15,200, and polymer **8** with a DP of 28 and M_n = 4,200. The disappearance of peaks corresponding to the epoxy group (C–O–C asymmetric

stretching 750–950 cm-1) in the IR spectrum (Figure S3) and the appearance of a broad peak at 3400–3700 cm^{-1} pertaining to the –OH stretching vibration (Figure S4 in the SI) confirmed quantitative epoxide ring-opening reaction. Furthermore, The NMR spectrum of **8.1** (Figure S6 in the SI) clearly shows the protons of pyridine ring at 7.3, 6.3 ppm, the shift of the proton adjacent to the oxirane ring and the appearance of the hydroxyl proton at 5.0 ppm. This suggests successful and quantitative conjugation of the HPO-ligands to the PGMA. In summary, fine-tuning of the structural features of the HPO ligands followed by RAFT-mediated PGMA preparation allowed the development of a small library of polymer-chelator materials with defined M_n and physico-chemical properties.

3.2 Determination of pKa and logKFe^{3+} values for hydroxypyridinones

The overall results for the five bidentate ligands are presented in Table 2. The pFe^{3+} values for **1**, **2, 4** and deferiprone are all similar, the slightly lower value for **3** results from the electron withdrawing influence of the β-amino function on the 1-substituent, which is para to one of the coordinating oxygens.

Table 2. Physico-chemical parameters of bidentate HPO-ligands.

	1	**2**	**3**	**4**	**5**	Deferiprone
pFe^{3+}	19.47	19.77	18.7	19.2	15.9	20.3
pKa_3	10.12	9.32	7.56	9.95	5.74	
pKa_2	9.72	6.62	9.68	9.03	9.17	9.77
pKa_1	3.45	1.41	3.09	3.14	3.99	3.68

The spectrophotometric titration of **1** is presented in SI (Figure S1 and S2). The pFe^{3+} of **5** is much lower than the other five HPOs and this is probably associated with the ability of **5** to exist in two tautomeric forms, one of which is catechol-like (Figure 2). Such tautomerism is not possible with the other analogues. Significantly the pFe^{3+} value for catechol is 15, which is close to that of **5**.

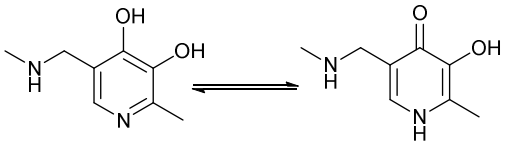

Figure 2. Tautomeric forms of compound **5**.

3.3 Characterization of bidentate-containing homopolymers

In order to evaluate the iron(III) binding properties of polymers, compounds **7.1** and **8.5** were selected as model compounds due to their different M_n and chelating units. UV–vis spectra of a range of solutions containing various polymer-iron(III) ratios were determined scanning between 300 and 600 nm (Figure 3 and SI Figure S13). Based on calculated M_n and number of chelating units per polymer chain (Table 1), the effective concentrations of the polymer-bound chelator on the homopolymers **7.1** and **8.5** were 81 and 172 µM. Bidentate iron chelators are known to form a 3:1 ligand:metal complexes with iron(III)[26]. As a consequence, it was expected that the metal complex saturation point for **7.1** and **8.5** would be reached at 27 and 57 µM Fe(III), respectively. In each polymer investigated the intensity of absorbance at 460 nm increased until a plateau. Indeed, the plateau for the polymer **7.1**: iron(III) curve is reached at around 27 µM iron(III) (Figure 3a), demonstrating that this polymer possesses high affinity for iron, and that all the chelating units appended to the PGMA backbone are available for metal binding.

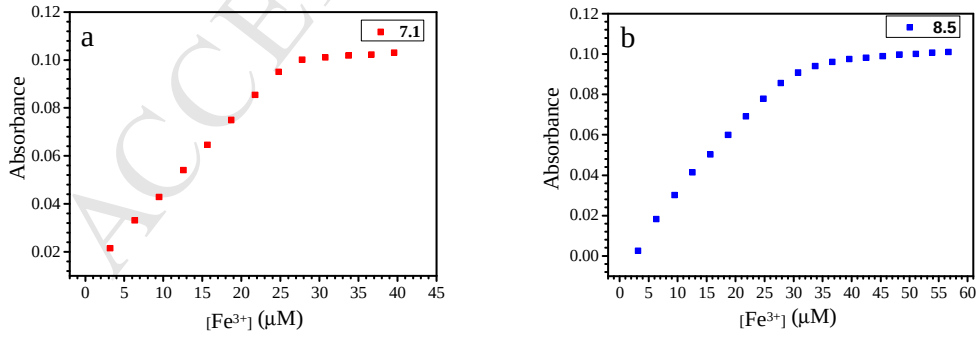

Figure 3. Plots of absorbance versus equivalent ratios of iron(III) to homopolymers **7.1** and **8.5** at 460 nm. The concentrations of homopolymers **7.1** and **8.5** were 0.75 and 6.15 µM, respectively. The solvent system was MOPS buffer.

In contrast, the saturation point for polymer **8.5** occurred at around 43 µM Fe(III), somewhat lower than the theoretical metal concentration (Figure 3b). This was attributed to the different metal chelator (namely compound **5**) attached to the PGMA in **8.5**. Such a chelator is conjugated much closer to the PGMA backbone, thus generating steric hindrance that may not permit efficient metal chelation[57]. Furthermore, the affinity for iron(III) is lower with this chelating unit when compared to **1**. The iron chelating capacities of **7.1** and **8.5** were calculated to be 843 and 350 µmolg, respectively. Thus the iron chelating capacity of the homopolymers in this study is greater than Chelex 100 (110 µmolg).[57]

Antibiotic susceptibility profile of the MRSA isolate

The isolate was seen to be resistant to only 4 of the 13 antibiotics used in this study (Table 3). Resistance of the isolate to Cefoxitin (10 µg), a β-lactam antibiotic, tentatively confirmed that the isolate was MRSA.

Table 3. Antibiotic susceptibility profile of the MRSA isolate used in this study

Antibiotics	**Susceptibility profile**
Cefoxitin (10 µg)	R
Linezolid (10 µg)	S
Fusidic acid (10 µg)	R
Tetracycline (10 µg)	S
Clindamycin (2 µg)	S
Ciprofloxacin (1 µg)	R
Neomycin (10 µg)	S
Erythromycin (5 µg)	R
Fosfomycin/Trometamol (200 µg)	S
Tigecycline (15 µg)	R
Quinupristin/Dalfopristin (15 µg)	S
Rifampicin (2 µg)	S
Gentamicin (10 µg)	S

R = Resistant, **S** = Susceptible

Identity of the isolate

The MRSA isolate used in this study was confirmed to be *S. aureus* as PCR amplification with primers nuc1 and nuc2 yielded an ~270 bp band of DNA (Figure 4) which corresponds to the nuc gene of *S. aureus*.

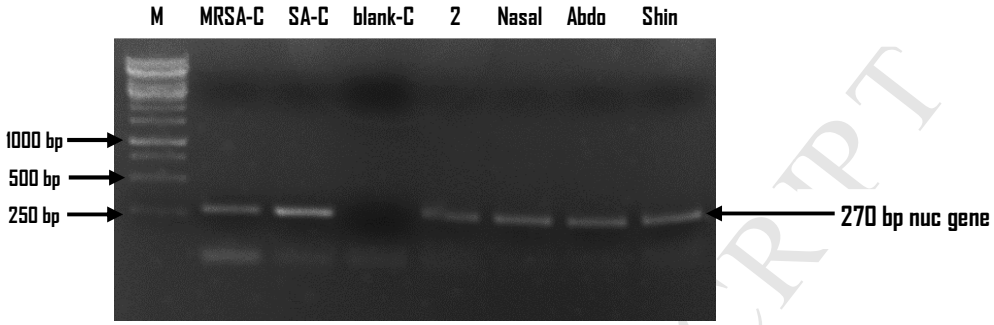

Figure 4. Gel showing products from PCR amplification of the ~270 bp *S. aureus*-specific nuc gene in four clinical MRSA isolates: **Lane M:** 1 kb Generuler; **Lane MRSA-C** = MRSA NCTC 12493 reference strain; **Lane SA-C** = *S. aureus* NCTC 6571 reference strain; **Lane blank C** = Blank control (PCR with no DNA). **Lanes 2, Nasal, Abdo and Shin:** Products obtained from the amplification of the nuc gene in six UK clinical MRSA isolates. *Nasal is the MRSA isolate used in this study

PCR amplification of a 162 bp *mecA* specific DNA using primers mec 1 and mec 2 in the MRSA isolate used in this study (as seen in Figure 5) conclusively confirmed that the isolate is indeed methicillin resistant.

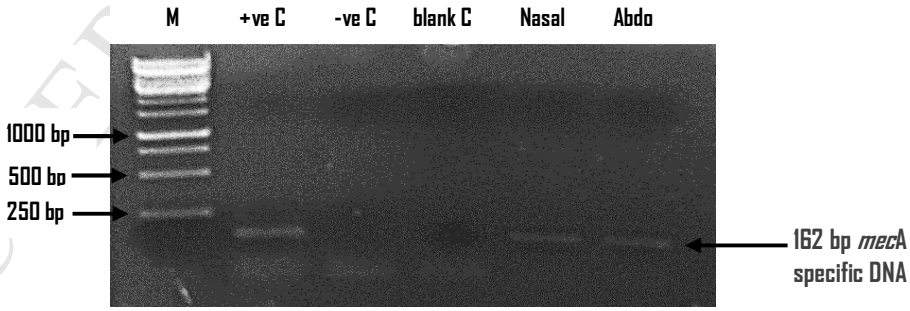

Figure 5. Gel showing products from PCR amplification of a 162 bp region of the *mecA* gene in two clinical *S. aureus* isolates: **Lane M:** 1 kb Generuler; **+ve C** = Positive control (MRSA NCTC 12493); **-ve C** = Negative control (*S. aureus* NCTC 6571); **blank C** = Blank control (PCR with no DNA); **Lanes Nasal and Abdo:** Products obtained from the amplification of the *mec*A specific DNA in both clinical MRSA isolates. *Nasal is the MRSA isolate used in this study

3.4 Antimicrobial effect of selected polymers on MRSA

In this work, we selected a range of polymers for biological evaluation, based on their physical properties such as M_n and acceptable solubility in water or aqueous DMSO systems, namely **7.1**, **7.5**, **8.1** and **8.5**.(Table 1). In addition, **7.5b** was evaluated as a non-chelating control to assess the importance of the iron-chelating activity of polymers with respect to their biological properties. The concentrations of the polymers used in this study are presented in Table 4. The inhibitory effects on MRSA are given in Figures 6 and 7 and their bactericidal effects are listed in Table 5. The number of viable cells was determined following incubation of bacteria for 24 hours in the presence and absence of various concentrations of the polymers. The greatest MRSA inhibitory effect was observed with **7.1**, which showed greater potency than **7.5**. Both polymers totally inhibited the growth of MRSA at 24 µM. **7.1** (12 µM) was found to exhibit a bactericidal rate of 100%. **7.1** is a more effective inhibitor of MRSA than **7.5** (MIC_**7.1** = <12µM; MIC_**7.5** = <24 µM) (Figure 6). This is in line with both their iron binding properties (Table 2) and their hydrophilicities, **7.1** being more hydrophilic than **7.5** (Table 1). The lower M_n counterparts of **7.1** and **7.5**, namely **8.1** and **8.5**, showed reduced bactericidal influence (Figure 7 and Table 5). Indeed, inhibitory effects for such polymers were only observed at concentrations above 48 µM. This suggests that the density of the chelating units on the macromolecular scaffold determines the potency of the compounds against MRSA. To further demonstrate that MSRA inhibition was derived by an iron-chelating mechanism, the control polymer **7.5b** was investigated and found to be much less effective at inhibiting MSRA growth than **7.5** (Figure 7 and Table 5). Polymer **7.5b** lacks iron-chelating ability due to methylation of phenolic moieties present on the HPO units. It is clear that the chelating properties of the active polymers are of sufficient strength to be able to compete with the growing microorganism for iron.

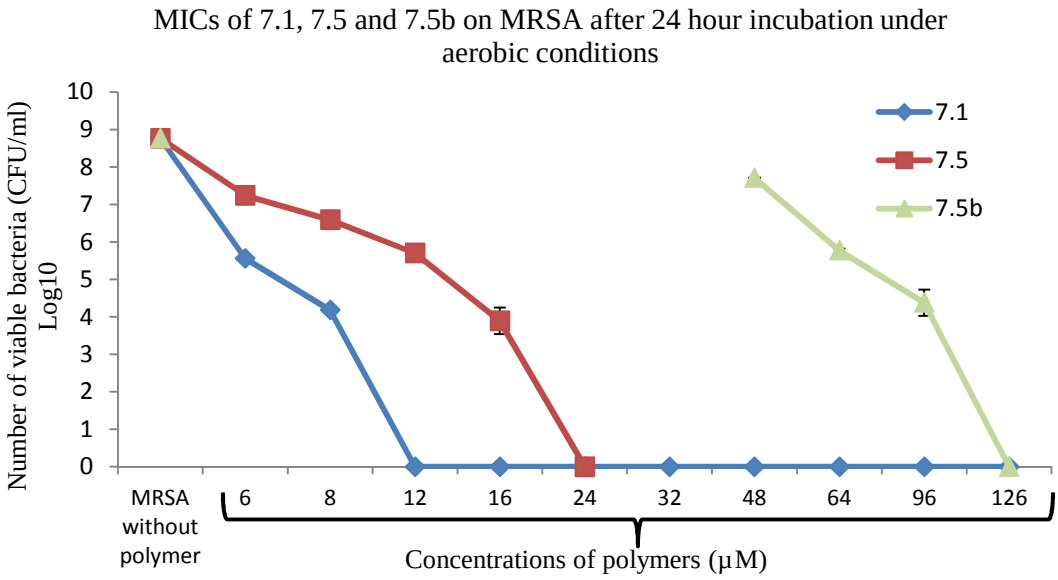

Figure 6. Antimicrobial effect of various concentrations of **7.1**, **7.5** and **7.5b** on MRSA after 24 hour incubation. Results are representatives of several independent experiments performed in duplicate. Error bars represent standard error.

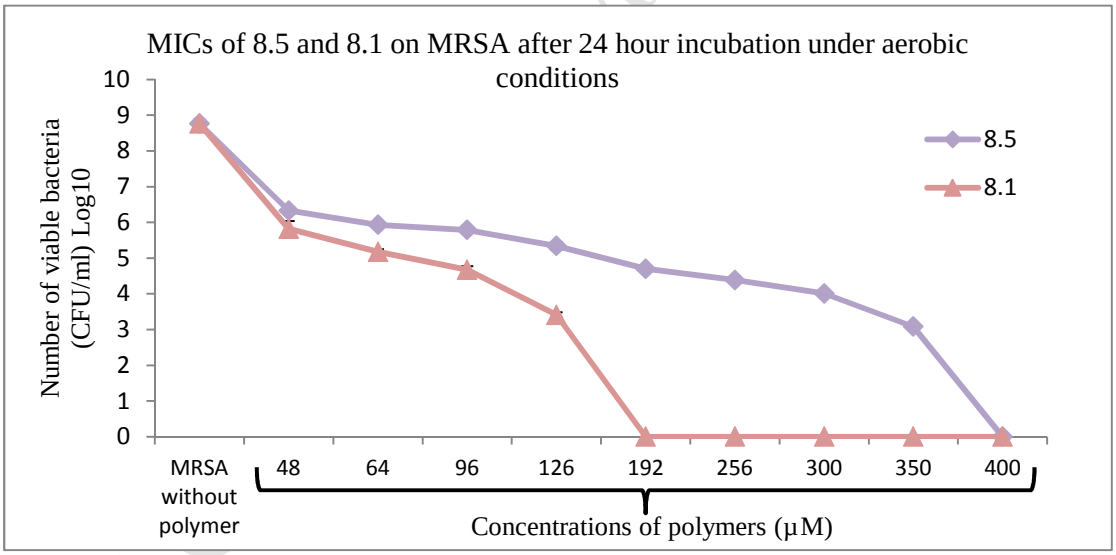

Figure 7. Antimicrobial effect of various concentrations of **8.5** and **8.1** on MRSA after 24 hour incubation. Results are representatives of several independent experiments, error bars represent standard error.

Table 4. Concentrations of the polymers used in the course of the study[1].

7.1 (M_n = 50,100)		**7.5** (M_n = 33,100)		**8.5** (M_n = 8900)		**7.0** (M_n = 34,600)		**8.1** (M_n = 13,400)	
µM	mg/mL	µM	mg/mL	µM	mg/mL	µM	mg/mL	µM	mg/mL
6	0.301	6	0.199	48	0.427	48	1.661	48	0.643
8	0.401	8	0.265	64	0.570	64	2.214	64	0.858
12	0.601	12	0.397	96	0.854	96	3.322	96	1.287
16	0.802	16	0.530	126	1.121	126	4.360	126	1.688
24	1.202	24	0.794	192	1.709	192	6.643	192	2.573
32	1.603	32	1.059	256	2.278	256	8.858	256	3.430
48	2.405	48	1.589	300	2.670	300	10.380	300	4.020
64	3.207	64	2.119	350	3.115	350	12.110	350	4.690
96	4.811	96	3.179	400	3.560	400	13.840	400	5.360

[1] MICs are highlighted in yellow

Table 5. Bacterial inhibition rate of various concentrations of polymers on MRSA after 24 hour incubation in an O_2 incubator.

7.1 (µM)	Bacterial inhibition rate after 24 hour incubation in an O_2 incubator (%)	**7.5** (µM)	Bacterial inhibition rate after 24 hour incubation in an O_2 incubator (%)	**8.5** (µM)	Bacterial inhibition rate after 24 hour incubation in an O_2 incubator (%)	**7.5b** (µM)	Bacterial inhibition rate after 24 hour incubation in an O_2 incubator (%)	**8.1** (µM)	Bacterial inhibition rate after 24 hour incubation in an O_2 incubator (%)
48	100	48	100	48	99.59942	48	91.12392	48	99.85187
32	100	32	100	64	99.85965	64	99.89625	64	99.97349
24	100	24	100	96	99.93199	96	99.99356	96	99.99144
16	100	16	99.99774	126	99.98988	126	100	126	99.99954
12	100	12	99.89395	192	99.99648	192	100	192	100
8	99.99735	8	99.31988	256	99.99927	256	100	256	100
6	99.93545	6	96.77233	300	99.99967	300	100	300	100
-	-	-	-	350	99.99979	350	100	350	100
-	-	-	-	400	100	400	100	400	100

4. Conclusions

RAFT polymerization of GMA in the presence of CPBD as the chain-transfer agent was adopted for the synthesis of PGMA with well-defined properties and low

polydispersities (PDI < 1.1). HPO-functionalized iron chelating homopolymers were synthesized by ring-opening reaction of RAFT-based PGMA using HPOs with various amine-substituents. The synthetic method is simple with high yield and low cost, and thus the approach could be applied to the syntheses of other related types of functional materials. The resulting materials possess different chelating capacity depending upon the type and amount of incorporated HPO. Water soluble, insoluble and/or fluorescent polymer-drug chimera are easily accessible using the described technology. The homopolymers showed high affinity for iron(III) and some were identified as new antimicrobial agents against MRSA. Polymer molecular weight and HPO ligand-type are important features in the determination of the potency of t macromoleculs for MRSA inhibition.

Supporting Information

Details of the synthesis and characterization of the HPO-ligands and iron-binding polymers are provided in the Supporting Information.

Corresponding Authors

* (V. A.) E-mail: vincenzo.abbate@kcl.ac.uk

* (G. Z) E-mail: gz6m@virginia.edu

Present Address

Institute of Pharmaceutical Science, King's College London, 150 Stamford Street, London SE1 9NH

Acknowledgement

The authors are grateful for financial support from National Natural Science Foundation of China (NSFC, 21222405).

References

1. Dhal PK, Polomoscanik SC, Avila LZ, Holmes-Farley SR, and Miller RJ. Advanced drug delivery reviews 2009;61(13):1121-1130.
2. Rossi NA, Mustafa I, Jackson JK, Burt HM, Horte SA, Scott MD, and Kizhakkedathu JN. Biomaterials 2009;30(4):638-648.
3. Mocioi M, Albu AM, Mateescu C, Voicu G, Rusen E, Marculescu B, and Mutihac L. Journal of Applied Polymer Science 2007;103(3):1397-1405.

4. Gorden AE, Xu J, Raymond KN, and Durbin P. Chemical Reviews 2003;103(11):4207-4282.
5. Lutfor M, Silong S, Yunus WW, Rahman M, Ahmad M, and Haron M. Journal of Chemical Research 2001;2001(8):326-327.
6. Tomita I, Mitsuhashi K, and Endo T. Journal of Polymer Science Part A: Polymer Chemistry 1996;34(2):271-276.
7. Tian F, Decker EA, and Goddard JM. Journal of agricultural and food chemistry 2012;60(8):2046-2052.
8. Tian F, Decker EA, and Goddard JM. Journal of agricultural and food chemistry 2012;60(31):7710-7718.
9. Lata S and Piehler J. Analytical Chemistry 2005;77(4):1096-1105.
10. Pramanik S, Dhara PK, and Chattopadhyay P. Talanta 2004;63(2):485-490.
11. Zhou T, Winkelmann G, Dai ZY, and Hider RC. Journal of Pharmacy and Pharmacology 2011;63(7):893-903.
12. Raad II, Fang X, Keutgen XM, Jiang Y, Sherertz R, and Hachem R. Current opinion in infectious diseases 2008;21(4):385-392.
13. Bergan T, Klaveness J, and Aasen AJ. Chemotherapy 2000;47(1):10-14.
14. Mahoney Jr J, Hallaway P, Hedlund B, and Eaton J. Journal of Clinical Investigation 1989;84(4):1362.
15. Hallaway PE, Eaton JW, Panter SS, and Hedlund BE. Proceedings of the National Academy of Sciences 1989;86(24):10108-10112.
16. Horowitz D, Margel S, and Shimoni T. Biomaterials 1985;6(1):9-16.
17. Winston A and Kirchner D. Macromolecules 1978;11(3):597-603.
18. Feng M-H, van der Does L, and Bantjes A. European Polymer Journal 1994;30(8):941-947.
19. Polomoscanik SC, Cannon CP, Neenan TX, Holmes-Farley SR, Mandeville WH, and Dhal PK. Biomacromolecules 2005;6(6):2946-2953.
20. Gao H, Lu X, Ma Y, Yang Y, Li J, Wu G, Wang Y, Fan Y, and Ma J. Soft Matter 2011;7(19):9239-9247.
21. Benaglia M, Alberti A, Giorgini L, Magnoni F, and Tozzi S. Polymer Chemistry 2013;4(1):124-132.
22. Yin H, Zheng H, Lu L, Liu P, and Cai Y. Journal of Polymer Science Part A: Polymer Chemistry 2007;45(22):5091-5102.
23. Zhu J, Zhou D, Zhu X, and Chen G. Journal of Polymer Science Part A: Polymer Chemistry 2004;42(10):2558-2565.
24. Li C, Yang Y-W, Liang Z-x, Wu G-l, and Gao H. Polymer Chemistry 2013;4(16):4366-4374.
25. An F, Gao B, Dai X, Wang M, and Wang X. Journal of hazardous materials 2011;192(3):956-962.
26. Zhou T, Ma Y, Kong X, and Hider RC. Dalton Transactions 2012;41(21):6371-6389.
27. Lowy FD. New England Journal of Medicine 1998;339(8):520-532.
28. Moellering RC. Journal of antimicrobial Chemotherapy 2011:dkr437.
29. Otto M. Cellular microbiology 2012;14(10):1513-1521.
30. Tattevin P, Schwartz BS, Graber CJ, Volinski J, Bhukhen A, Bhukhen A, Mai TT, Vo NH, Dang DN, and Phan TH. Clinical infectious diseases 2012:cis527.
31. Chu VH, Crosslin DR, Friedman JY, Reed SD, Cabell CH, Griffiths RI, Masselink LE, Kaye KS, Corey GR, and Reller LB. The American journal of medicine 2005;118(12):1416. e1419-1416. e1424.
32. Boucher HW and Corey GR. Clinical infectious diseases 2008;46(Supplement 5):S344-S349.
33. Thwaites GE and Group UKCIR. PLoS One 2010;5(12):e14170.
34. Filice GA, Nyman JA, Lexau C, Lees CH, Bockstedt LA, Como-Sabetti K, Lesher LJ, and Lynfield R. Infection Control 2010;31(04):365-373.
35. Crisóstomo MI, Westh H, Tomasz A, Chung M, Oliveira DC, and de Lencastre H. Proceedings of the National Academy of Sciences 2001;98(17):9865-9870.
36. Scanvic A, Denic L, Gaillon S, Giry P, Andremont A, and Lucet J-C. Clinical infectious diseases 2001;32(10):1393-1398.

37. Chambers HF. Emerging infectious diseases 2001;7(2):178.
38. Klein E, Smith DL, and Laxminarayan R. Emerging infectious diseases 2007;13(12):1840.
39. DeLeo FR and Chambers HF. The Journal of clinical investigation 2009;119(9):2464.
40. Gould I, Reilly J, Bunyan D, and Walker A. Clinical Microbiology and Infection 2010;16(12):1721-1728.
41. Löffler B, Hussain M, Grundmeier M, Brück M, Holzinger D, Varga G, Roth J, Kahl BC, Proctor RA, and Peters G. PLoS pathogens 2010;6(1):e1000715.
42. Chatterjee SS and Otto M. Clinical epidemiology 2013;5:205.
43. Mohr JF and Murray BE. Clinical infectious diseases 2007;44(12):1536-1542.
44. Yang Y, McBride MV, Rodvold KA, Tverdek F, Trese AM, Hennenfent J, Schiff G, Lambert BL, and Schumock GT. American Journal of Health-System Pharmacy 2010;67(12):1017-1024.
45. Gould IM, David MZ, Esposito S, Garau J, Lina G, Mazzei T, and Peters G. International journal of antimicrobial agents 2012;39(2):96-104.
46. Rodvold KA and McConeghy KW. Clinical infectious diseases 2014;58(suppl 1):S20-S27.
47. Qiu DH, Huang ZH, Zhou T, Shen C, and Hider RC. FEMS Microbiology Letters 2011; 314: 107–111.
48. Zhou YJ, Liu MS, Osamah AR, Kong XL, Alsam S, Battah S, Xie YY, Hider RC and Zhou T. European Journal of Medicinal Chemistry 2015; 94: 8– 21.
49. Keddie DJ. Chemical Society Reviews 2014;43(2):496-505.
50. Harrisson S, Liu X, Ollagnier J-N, Coutelier O, Marty J-D, and Destarac M. Polymers 2014;6(5):1437-1488.
51. Gans P and O'Sullivan B. Talanta 2000;51(1):33-37.
52. Gans P, Sabatini A, and Vacca A. Annali di chimica 1999;89(1-2):45-49.
53. Andrews JM. Journal of antimicrobial Chemotherapy 2001;48(suppl 1):5-16.
54. Dobbin PS, Hider RC, Hall AD, Taylor PD, Sarpong P, Porter JB, Xiao G, and van der Helm D. Journal of medicinal chemistry 1993;36(17):2448-2458.
55. Rai BL, Dekhordi LS, Khodr H, Jin Y, Liu Z, and Hider RC. Journal of medicinal chemistry 1998;41(18):3347-3359.
56. Piyamongkol S, Ma YM, Kong XL, Liu ZD, Aytemir MD, van der Helm D, and Hider RC. Chemistry-A European Journal 2010;16(21):6374-6381.
57. Zhou T, Kong XL, Liu ZD, Liu DY, and Hider RC. Biomacromolecules 2008;9(5):1372-1380.
58. Ma Y, Luo W, Camplo M, Liu Z, and Hider RC. Bioorganic & Medicinal Chemistry Letters 2005;15(14):3450-3452.
59. Kim HN, Guo Z, Zhu W, Yoon J, and Tian H. Chemical Society Reviews 2011;40(1):79-93.
60. Willcock H and O'Reilly RK. Polymer Chemistry 2010;1(2):149-157.

Highlights

·HPO-functionalized iron chelating polymers were synthesized from RAFT-based PGMA.

·The synthetic method of the resulting materials is simple with high yield and low cost.

·Homopolymers were identified as new antimicrobial agents against MRSA.

·This versatile synthetic procedure can be adopted to prepare a wide range of polymeric chelators.